NANO LETTERS

Letter

pubs.acs.org/NanoLett

Temporary Charge Carrier Separation Dominates the Photoluminescence Decay Dynamics of Colloidal CdSe Nanoplatelets

Freddy T. Rabouw,*[,†] Johanna C. van der Bok,[†] Piernicola Spinicelli,[‡] Benoît Mahler,[‡] Michel Nasilowski,[‡] Silvia Pedetti,[‡] Benoît Dubertret,[‡] and Daniël Vanmaekelbergh[†]

[†]Condensed Matter and Interfaces, Debye Institute for Nanomaterials Science, Princetonplein 1, 3584 CC Utrecht, The Netherlands

[‡]Laboratoire de Physique et d'Etude des Matériaux (LPEM), PSL Research University, ESPCI-ParisTech, 10 rue Vauquelin, F-75231 Paris Cedex 5, France

Supporting Information

ABSTRACT: Luminescent colloidal CdSe nanoplatelets with atomically defined thicknesses have recently been developed, and their potential for various applications has been shown. To understand their special properties, experiments have until now focused on the relatively short time scales of at most a few nanoseconds. Here, we measure the photoluminescence decay dynamics of colloidal nanoplatelets on time scales up to tens of microseconds. The excited state dynamics are found to be dominated by the slow ($\sim\mu$s) dynamics of temporary exciton storage in a charge-separated state, previously overlooked. We study the processes of charge carrier separation and exciton recovery in pure CdSe nanoplatelets as well as in core–crown and core–shell CdSe/CdS nanoplatelets with high ensemble quantum yields of 50%, and discuss the implications. Our work highlights the importance of reversible charge carrier trapping and experiments over a wide range of time scales for the understanding of colloidal nanoemitters in general and nanoplatelets in particular.

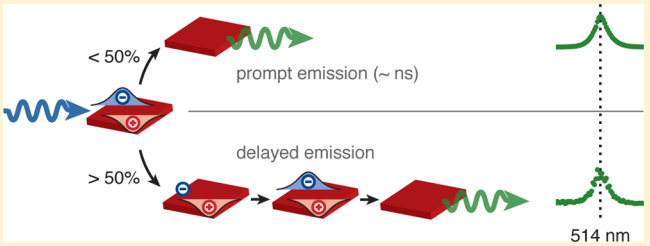

KEYWORDS: *Colloidal nanoplatelets, photoluminescence decay, exciton recombination, charge carrier trapping*

Traditionally, the research on luminescent semiconductor nanocrystals has focused on spherical nanocrystals (also known as quantum dots) or rod-shaped nanocrystals. Recently, colloidal nanoplatelets (NPLs) of CdSe with atomically defined thickness have become popular.[1−5] These NPLs have been reported to exhibit remarkable optical properties, different from those of spherical and rod-shaped luminescent nanocrystals. Most importantly, the NPLs have narrower ensemble emission spectra[2] and have been reported to exhibit faster spontaneous emission.[6] Narrow spectra arise because the emission wavelength of a NPL is mainly determined by its atomically defined thickness, which can be the same for all NPLs in an ensemble.[1,6] The fast photoluminescence (PL) decay, as observed from time-resolved spectroscopy, has been ascribed to a "giant oscillator strength" effect, that is, the radiative decay enhancement due to 2D motion of the exciton.[6,7]

Several promising applications of colloidal NPLs have been demonstrated, for example as electroluminescent material in light-emitting diodes,[8,9] as gain material in lasers,[10] as photodetector,[11] or as photocatalyst.[12] Despite the many potential applications of colloidal NPLs, experimental studies on the fundamental properties have until now focused on processes occurring on time scales of a few nanoseconds or faster. For example, extensive studies have been performed on decay pathways of the single-exciton state,[6,13,14] the exciton fine structure at cryogenic temperature,[15] nonradiative Auger recombination[10,16,17] or transfer of the excitated state energy.[18−20] Slower PL decay components up to a few 100 ns have been observed and mentioned in some of the previous studies,[18,22,23] but have not been investigated in detail.

Here, we show that the decay dynamics of NPLs are in fact dominated by much slower decay than previously investigated. Following excitation, there is a more than 50% probability that one of the charge carriers is temporarily trapped. Eventually, this carrier is released and recombines under the emission of a photon of the same energy as the prompt emission (i.e., the immediate radiative decay). This gives rise to "delayed emission" on time scales of up to tens of microseconds. Indeed, examining previously reported PL decay curves of NPLs, we see that the PL never reaches a flat background on the short time scales analyzed until now.[6,13,14,16,17,19,22] We compare the PL decay dynamics of NPLs of pure CdSe to core–crown and core–shell geometries of CdSe/CdS with ensemble PL quantum yields of ~50%. For all three batches, the decay is strongly multiexponential and the contribution of delayed emission to the total emission of NPLs is more than 50%, considerably higher than for spherical quantum dots.[24−26] At the same time, we find that the energy spectrum of delayed emission is the same as that of prompt emission, and as narrow.

Received: January 5, 2016
Revised: February 9, 2016
Published: February 11, 2016

DOI: 10.1021/acs.nanolett.6b00053
Nano Lett. 2016, 16, 2047−2053

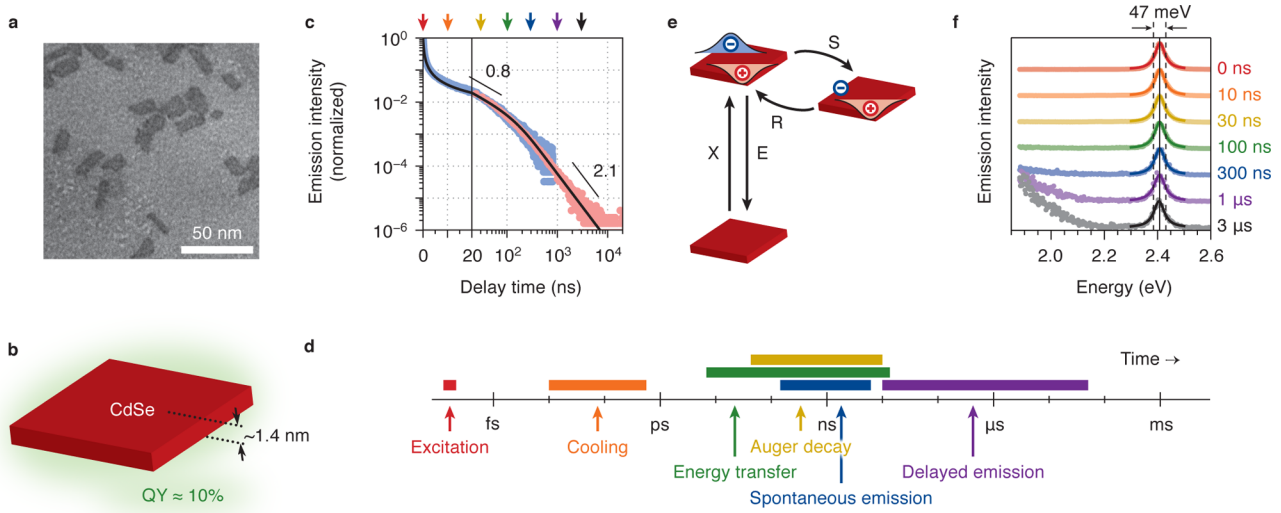

Figure 1. (a) A TEM image of the CdSe NPLs investigated. They are roughly 10 nm × 20 nm in lateral extension. (b) Schematic representation of a core-only CdSe NPL with an ensemble quantum yield of ~10% centered at 514 nm (Supporting Information, Figure S1) and an atomically defined thickness of approximately 1.4 nm.[3] (c) The PL decay of the NPLs (detected at 514 nm) dispersed in toluene is plotted on a semilogarithmic scale on the first 20 ns, and on a double-logarithmic scale from 20 ns to 20 μs. The blue and red data points are from separate measurements at different time resolutions and with different laser repetition rates but similar pulse fluence. (d) The time scales involved in the excited state dynamics of NPLs range from subpicoseconds at which charge carrier cooling occurs[27] to the microseconds dynamics of "delayed emission" investigated here. Previous work has focused on the picoseconds to nanoseconds time scales, where energy transfer[18−20] and Auger recombination[10,16,17] occur, as well as the initial stages of single-exciton decay.[6,10,13−15,18] (e) A model of charge carrier separation (S) and release (R) explains power-law delayed emission.[24] The timing of emission is determined by charge carrier release (R) whereas the energy is set by the exciton recombination process (E). (f) Emission spectra at varying delay time after excitation reveal that the band shape due to exciton recombination (at 2.42 eV = 514 nm) remains constant. Arrows in panel c mark the delay times for which spectra are plotted.

This is consistent with the model of temporary charge carrier trapping followed by full restoration of the exciton state. Our results improve the understanding of an emerging class of luminescent materials, demonstrating that a previously overlooked process dominates the excited state dynamics.

Delayed Emission from Core-Only Nanoplatelets. We first study NPLs consisting purely of CdSe, that we call "core-only" NPLs. They are approximately 10 nm × 20 nm in lateral extension (Figure 1a). The emission is centered at 514 nm (Supporting Information, Figure S1) from which we know that the NPLs have a thickness of ~1.4 nm (Figure 1b).[3] The emission band is as narrow as 8 nm full width at half-maximum (fwhm) because there is no inhomogeneous broadening due to polydispersity in the NPL thickness.[22]

In Figure 1c, we show the PL decay dynamics of core-only NPLs upon pulsed excitation at 441 nm. The first 20 ns is plotted on a semilogarithmic scale, and we see multiexponential decay with a subnanosecond fastest component. Previous studies have investigated the excited state dynamics of NPLs on this time scale or shorter[6,10,13−20,27] (Figure 1d). The PL lifetimes reported for the single-exciton state are typically a few nanoseconds[6,14,16,18] or even subnanosecond,[10,13−16] much shorter than encountered for spherical quantum dots (20−30 ns). Such fast dynamics in NPLs have been ascribed to accelerated radiative decay due to the "giant oscillator strength" effect.[6,7] Here, we continue the PL decay measurements until 20 μs after excitation, as plotted in Figure 1c on a double-logarithmic scale. In Supporting Information Figure S3, we present plots of the full PL decay curve on semilogarithmic or double-logarithmic scales.

The photon count rate drops an order of magnitude in the first 3 ns after excitation (Figure 1c), which is why CdSe NPLs are generally associated with fast excited state dynamics.[6,10,13−20] We see now, however, that at times beyond a few nanoseconds the decay slows down. This slow-down is so significant that the majority of the photons is in fact emitted later than 5 ns after excitation (see further Figure 3a,b) with power-law decay dynamics. The solid line is a fit to an exponential prompt emission component plus two power-law components (see Methods). This model matches the data much better than a multiexponential fit (Supporting Information, Figure S5). "Delayed emission" on time scales much longer than the intrinsic lifetime of the single-exciton state has been ascribed to temporary charge carrier trapping, until eventual release of the trapped charge resulting in emission (Figure 1e).[24−26,28] Indeed, release and radiative recombination of trapped charges in CdSe NPLs is also observable in thermoluminescence experiments.[29]

Figure 1f shows the emission spectra of the core-only NPLs at varying delay time from the first nanoseconds (red) to 3 μs after excitation (gray). The solid lines are Lorentzian fits of the line shape (on energy scale; see Supporting Information Figure S2), from which we extract the peak positions and widths. Both parameters are constant to within 1 meV over the course of the experiment (Supporting Information, Figure S4). Indeed, the emission line shape of the delayed exciton recombination (orange to black data points in Figure 1f) is the same as in the initial spectrum (0 ns delay time, red). At the latest delay times of 1 and 3 μs, we observe an additional emission band at low energy, which can be ascribed to direct recombination of deeply trapped charge carriers. In the Supporting Information Figure S8, we show the dynamics of this trap emission.

As discussed in more detail in Figure 3a,b, the excited state decay of CdSe NPLs contains lifetime components covering at least 4 orders of magnitude with the majority of photons emitted later than 10 ns after excitation. On the other hand, the

DOI: 10.1021/acs.nanolett.6b00053
Nano Lett. 2016, 16, 2047−2053

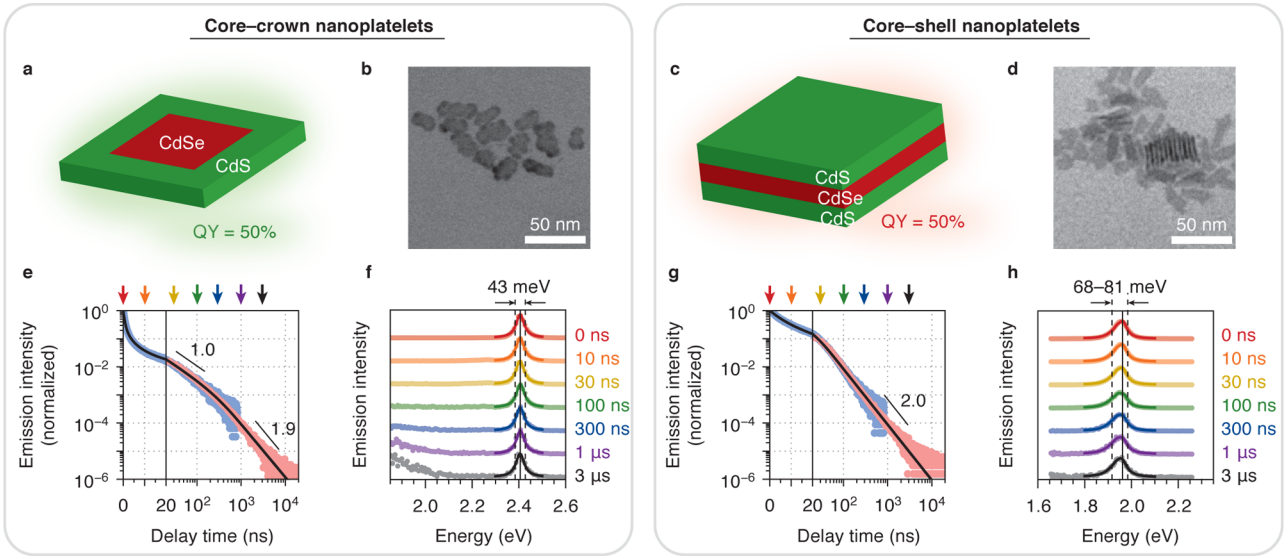

Figure 2. (a) A cartoon and (b) TEM image of the core–crown NPLs investigated.[5] They emit green light of 514 nm, as the core-only NPLs, but with a higher PL QY of approximately 50%. (c) A cartoon and (d) TEM image of the core–shell NPLs investigated.[3] Compared to core-only NPLs, the emission is red-shifted to 635 nm because quantum confinement in the thin direction of the NPL is weakened. (e) The PL decay dynamics of the core–crown NPLs (detected at 514 nm), as well as (f) the time-resolved emission spectra, are nearly identical to the core-only NPLs. The solid lines in panel f are Lorentzian fits (see Supporting Information, Figures S2 and S4). (g) On the first 20 ns, the PL decay of core–shell NPLs is slower than that of core-only and core–crown NPLs. At late times, however, the delayed emission is equally intense and exhibits similar power-law statistics. (h) The time-resolved spectra of the core–shell NPLs can be fitted to a series of Lorentzian phonon replicas due to phonon coupling (solid lines; see Supporting Information Figure S2).[22]

emission spectrum of the NPL ensemble is exceptionally narrow over the whole time range. The seemingly counter-intuitive combination of widely distributed dynamics and narrow energetics can be understood from the model of charge carrier trapping and release (Figure 1e). The dynamics and energetics are determined by different physical processes, namely the release of the trapped charge (process R) and photon emission by exciton recombination (process E), respectively.

The experimental results presented above demonstrate a major effect of temporary charge carrier trapping on the decay dynamics of CdSe NPLs. While in spherical QDs we have previously shown that "delayed emission" following temporary exciton storage by charge carrier trapping constitutes 10%–25% of the total emission[24] (as determined from a fit of an exponential and a power-law contribution to the PL decay), in the NPLs here this number is of the order of 50%. Indeed, terahertz measurements have previously revealed significant charge carrier trapping in CdSe NPLs.[14] Our result here is in agreement with those of multiexponential fits by Olutas et al. on time scales up to several 100 ns.[23] The contribution of delayed emission is in fact so large that there is no clear transition from the exponential decay component due to immediate exciton recombination and the power-law component due to delayed emission. In contrast to spherical quantum dots,[24] the delayed contribution in the emission of NPLs is therefore more difficult to quantify precisely. Previous studies have achieved prolonged but reversible exciton storage in CdSe/CdS dot-in-rods[30] or tetrapods[31] using external electric fields. In the NPLs examined here, temporary exciton storage occurs spontaneously but can possibly be controlled with external fields.

High Quantum Yield Core–Shell and Core–Crown NPLs. Charge carrier traps are usually associated with low-quality quantum dots. Indeed, charge carrier traps are often considered responsible for nonradiative charge carrier recombination leading to low PL quantum yields (QYs). The core-only NPLs investigated above have a reasonable QY of 10% (measured with the integrating sphere at an absorbance of ~30%). Next, we investigate two batches of NPLs with five times higher QYs of approximately 50%. They are CdSe/CdS core–crown[5] and core–shell NPLs[3] (see Figure 2a–d for cartoons and TEM images) that were grown from the core NPLs of Figure 1.

The PL decay dynamics (Figure 2e) and energetics (Figure 2f) of core–crown NPLs are nearly identical to those of the core-only NPLs (Figure 1). Although the QY is five times higher, the contribution of delayed emission to the total PL is as high. Hence, the nonradiative decay pathways leading to a relatively low QY of the core-only NPLs are seemingly unrelated to the temporary charge carrier trapping resulting in delayed emission. This suggests that the traps responsible for delayed emission are not centers for nonradiative recombination. Instead, they have a high probability to eventually release the charge carriers, thereby restoring the emissive exciton state. The 5× higher ensemble QY of the core–crown NPLs can be explained with the concept of a "dark fraction" of emitters:[32−34] "bright" NPLs have a high QY and generate the PL decay curve, while "dark" NPLs have a QY so low that they are invisible in PL decay experiments. Consequently, the PL decay dynamics as observed, including the strong delayed component, are intrinsic to bright NPLs. The difference in QY between core-only and core–crown NPLs is then due to a different distribution between dark and bright NPLs. Apparently, the growth of a CdS crown on a dark CdSe NPL can eliminate nonradiative recombination centers and make the NPL bright, without affecting the traps responsible for delayed emission.

We note that the observation of very similar PL decay dynamics of core-only and core–crown NPLs does not necessarily mean that the excited-state dynamics of each

DOI: 10.1021/acs.nanolett.6b00053
Nano Lett. 2016, 16, 2047−2053

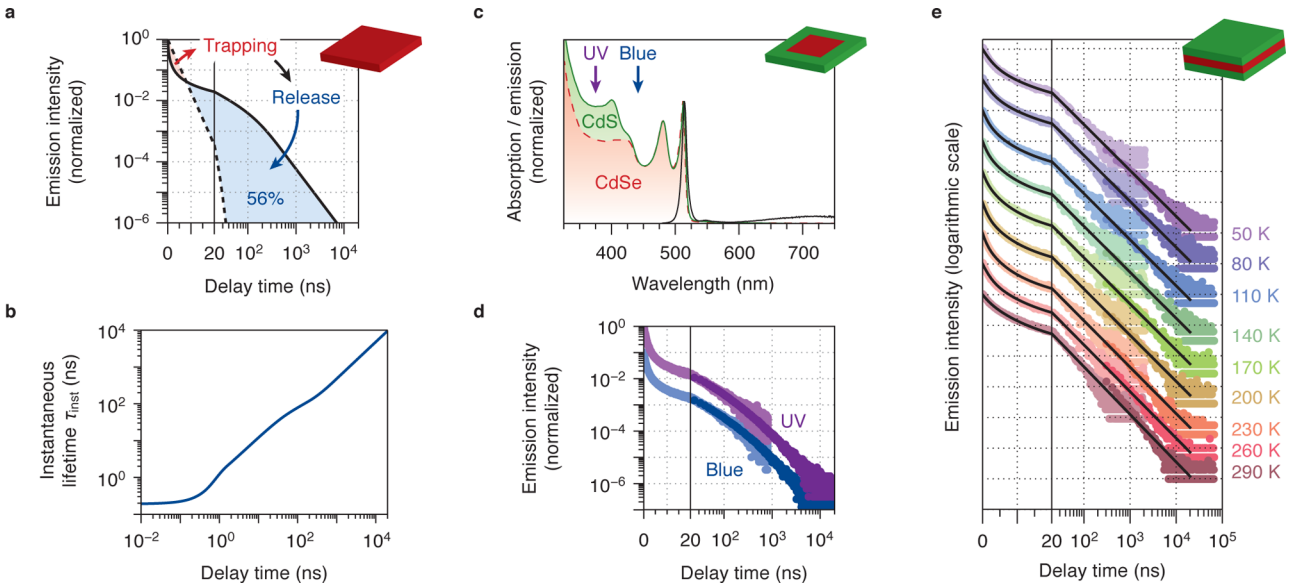

Figure 3. (a) The PL decay dynamics of core-only CdSe NPLs (solid line is the fit from Figure 1c) are multiexponential due to charge carrier separation and release. The dashed line is a single-exponential decay curve with the same integrated area, representing the scenario where charge carrier separation and release do not occur. We see that the true decay is faster in this scenario initially because of charge carrier separation but slower after 8 ns because of charge carrier release. (b) The instantaneous lifetime of the core-only CdSe NPLs, $\tau_{inst}(t) = I(t)/I'(t)$, as a function of delay time. (c) The absorption (green) and emission (black) of core−crown NPLs. The dashed red line is the absorption spectrum of core-only NPLs. The difference between the two absorption spectra is due to absorption in the CdS crown. (d) The PL decay curves of the core−crown NPLs upon excitation at 441 nm (blue; exciting in the CdSe core; data shifted by a factor 10) and upon excitation at 375 nm (purple; exciting both core and crown) are nearly identical. (e) Temperature-dependent PL decay of the core−shell NPLs, up to 80 μs after excitation at 402 nm. Each next measurement is offset by a factor 10. The light- and dark-colored data points are two different sets of measurements at different excitation powers and time resolutions. The black lines are fits to an exponential prompt decay component plus a power-law delayed component (see Supporting Information Figure S8d,e).

individual "bright" NPL are exactly the same. There may be some variation of the rate constants involved. Nevertheless, the similarity of the ensemble-averaged PL decay dynamics suggests that reversible trapping with power-law delayed emission dynamics is an intrinsic property of a bright NPL. Indeed, previous experiments have revealed multiexponential decay on the single-NPL level.[21,22] Future PL decay experiments on individual NPLs at low repetition rate will have to quantify the inhomogeneity in the statistics of reversible trapping.

The core−shell NPLs show different characteristics (Figure 2g,h) than the core-only and the core−crown NPLs. The emission energy is lower by 460 meV, and the spectrum is broader by ~30 meV (Figure 2h). These differences are due to delocalization of the charge carriers into the CdS shell: the quantum confinement energy is lower in core−shell NPLs (leading to a lower emission energy) and exciton−phonon coupling increases[22] (leading to a broader spectrum). Phonon coupling, parametrized by the Huang−Rhys parameter,[35] is stronger for delayed emission than for prompt emission (see Supporting Information, Figure S4). As a result, the spectrum broadens slightly (from 68 meV fwhm initially to 81 meV) over the course of 3 μs. An explanation for this may be some inhomogeneous spectral broadening due to variations in the CdS shell thickness.[22] NPLs with a thicker CdS shell might have a slightly different probability of reversible charge carrier trapping,[24] and therefore more strongly contribute to the delayed emission.

We also see that the PL decay of core−shell NPLs on the first 20 ns is slower (Figure 2h) than in core-only and core−crown NPLs. This means that the rates of prompt decay (radiative and trapping) are slower, because of exciton delocalization. The delayed emission from core−shell NPLs on time scales after 100 ns is nevertheless similar to that from core-only and core−crown NPLs: the intensity is similar, as well as the power-law slope. Therefore, although the fastest trapping and release processes are absent or hidden by the slower dynamics of initial decay (compare the numbers provided in the Supporting Information, Figure S6), the probability of reversible charge carrier trapping on time scales slower than 100 ns is as high as in core-only and core−crown NPLs.

Summarizing the comparison between the different samples of NPLs, we have confirmed that a protective CdS shell on the NPLs prevents nonradiative recombination and increases the ensemble QY.[3,5] However, temporary charge carrier traps are active irrespective of whether the surface of NPLs is protected and seemingly independent of the ensemble QY. This may mean that the traps are in fact intrinsic to CdSe or that they are present in equal density on the outer surface of a CdSe crystal or on a CdSe/CdS interface. Atomistic quantum mechanical calculations are necessary to give a definite answer on this point.[36]

Charge Carrier Trapping and Release. In the next part of this work, we further investigate the process of charge carrier separation and release in the three samples. The black solid line in Figure 3a shows the PL decay dynamics of the core-only NPLs, reproduced from Figure 1c. A total of 4.2 million photons were recorded over 10 min. As shown above, the strongly multiexponential character of the decay is due to reversible trapping without nonradiative losses. With the dashed line, we simulate a single exponential decay curve that yields the same number of photons (i.e., the same integrated

DOI: 10.1021/acs.nanolett.6b00053
Nano Lett. 2016, 16, 2047−2053

area). This represents the hypothetical situation where temporary trapping (S and R in Figure 1e) is not active, that is, the excitons are not temporarily stored. In other words, the dashed line depicts the radiative prompt component (E in Figure 1e) of the decay of the NPLs. The single-exponential lifetime of the curve is $\tau = \int I(t)dt/I(0) = 2.5$ ns (where $I(t)$ is the fitted emission intensity at delay time t). By comparing the solid and dashed lines we can directly see how trapping causes acceleration of the initial decay on the first 8.0 ns (red-shaded area; over the first 5 ns and the first decade of intensity decay), while release of the trapped charge carriers results in a slow-down on later time scales (blue-shaded area). As many as 56% of the photons come out later than they would if temporary charge carrier trapping did not occur. This means that at least 56% of the emission is preceded by exciton storage for 8 ns or longer. The remaining 44% may involve temporary trapping for times so short that there is no significant effect on the emission dynamics, but the frequency of these events is hard to quantify because the radiative lifetime of the NPLs is not known. In the Supporting Information, Figure S6 we perform the analysis of Figure 3a on the core−crown and core−shell NPLs.

Figure 3b illustrates how widely distributed the time scales of delayed emission are. We plot the "instantaneous lifetime", that we define as $\tau_{inst}(t) = I(t)/I'(t)$ (with $I'(t)$ as the time derivative of the fitted emission intensity). This parameter is a measure for the slope of the PL decay curve and represents the lifetime components contained in it (see also Supporting Information, Figure S5b). The instantaneous lifetime is initially 0.2 ns, consistent with previously reported fast lifetime components of NPLs.[10,13,15,16,23] Indeed, NPLs may seem to be "fast emitters"[6,10,13−15,18] on time scales up to 10 ns. However, we see that the decay also contains components of 10 μs, 5 orders of magnitude slower. These slow processes must be considered for a full understanding of the excited state dynamics of colloidal NPLs.

The core−crown NPLs are exceptionally suitable to investigate the effect of excitation wavelength. The CdSe core absorbs at wavelengths shorter than 514 nm (red dashed line in Figure 3c; the absorption spectrum of the core-only NPLs) while the CdS crown only absorbs at wavelengths shorter than ~420 nm (green line in Figure 3c; the absorption spectrum of the core−crown NPLs). Figure 3d shows that the PL decay curve recorded while exciting in the CdSe core (blue; 441 nm) is indistinguishable from that obtained when exciting in the CdS crown (UV; 375 nm). Also for the core-only and core−shell NPLs, there is no effect of the excitation wavelength (Supporting Information, Figure S7). We conclude that charge carrier separation by the traps responsible for delayed emission is slower than localization in the CdSe core. Indeed, charge carrier cooling[37] and localization[38] typically occurs on subpicosecond time scales in CdSe/CdS heteronanocrystals.

Finally, we examine the effect of temperature down to 50 K on delayed emission. The NPLs were drop-cast on an alumina coverslip, dried, and measured in vacuum in a cryostat. After sample preparation, PL from the core-only and core−crown NPLs is partially quenched and the dynamics are faster compared to solution measurements (see Supporting Information, Figure S9). These effects may result from concentration quenching by energy transfer between NPLs[18,19] or permanent charging.[39] The core−shell NPLs are not affected by quenching so much. In Figure 3e, we show the temperature dependence of the decay dynamics of the core−shell NPLs. The fitted initial decay rate and the power-law slope of delayed emission change a little with temperature (Supporting Information, Figure S9d,e). However, qualitatively the delayed emission dynamics are similar over the full temperature range of a factor six in absolute temperature.

Interestingly, temperature-independence of power-law statistics has also been found for blinking from single CdSe quantum dots,[40,41] confirming the notion that blinking and delayed emission must share the same physical origin.[24,25] Models to explain temperature-independent charge carrier trapping and release have been proposed before in the framework of blinking. For example, charge carrier trapping and release could occur via tunneling processes. This means that the system does not go over, but through the energy barrier separating the normal and the charge separated states. The power-law statistics would result from temporal variations in the width and/or height of the tunneling barrier.[40,41] Alternatively, trapping and release could occur resonantly, where the power-law statistics arise from "spectral" diffusion of the energies of the neutral and charge-separated states of the emitter.[42,43]

Discussion. Previous experiments have focused on time scales of a few nanoseconds or faster[6,10,13−20,27] and have therefore overlooked delayed emission from NPLs that occurs on time scales up to tens of microseconds (Figures 1 and 2). Here, we have shown that temporary charge carrier separation, followed by recovery of the exciton state, leads to strong delay in the emission. More than 50% of the photons (blue area in Figure 3a) are emitted later than after 8 ns, because of exciton storage in a nonemissive charge-separated state. This charge-separated state must therefore form with a high probability of at least 50% within the first few ns after excitation (red area in Figure 3a).

What do our results imply for the understanding of colloidal CdSe-based NPLs? First, there seems to be no correlation between the occurrence of delayed emission and ensemble QY. As discussed above, this implies that the charge carrier traps responsible for delayed emission are not centers for non-radiative recombination. While the charge-separated state persists, however, a NPL may be dark because of Auger quenching, that is, excitations during the charge-separated state do not lead to emission. We have previously proposed that this can lead to a lower ensemble-averaged QY at high excitation powers as well as blinking.[24] More experiments are necessary to directly relate delayed emission to blinking and PL at high excitation powers.

Decay of NPLs on nanosecond time scales is commonly interpreted in terms of fast radiative decay[6,10,13−15,18] and energy transfer[18−20] at low excitation power or Auger recombination[10,16,17] at higher excitation powers. We conclude here that the radiative lifetime of CdSe NPLs is on the order of a few ns. The occurrence of (reversible) charge carrier trapping makes the observed lifetime even shorter than this, but the carriers are released at later times. Indeed, Kunneman et al.[14] have recently proposed a model of charge carrier trapping to explain the discrepancy between PL and transient absorption measurements on NPLs. However, in their model charge carrier trapping is not reversible but leads to nonradiative recombination. Including the release of trapped charge carriers would certainly affect their model. Similarly, reversible charge carrier trapping would most likely affect the interpretation of previous experiments on energy transfer and Auger recombination in NPLs.[10,16−20] For example, fast but temporary charge carrier trapping may protect biexciton states from Auger quenching. It

DOI: 10.1021/acs.nanolett.6b00053
Nano Lett. 2016, 16, 2047−2053

may also enable energy transfer from and between NPLs by means of sequential charge transfer rather than Förster energy transfer.

Conclusion. To summarize, we have examined PL from CdSe NPLs and CdSe/CdS core–crown and core–shell NPLs up to microsecond time scales. Dynamics slower than 10 ns dominate the PL decay but have been overlooked in previous experiments. They arise from a high probability of more than 50% that absorption of a photon is followed by temporary charge carrier trapping. Interestingly, this temporary trapping is not directly related to PL quenching. The emission line shape remains narrow over the full time scale up to microseconds, because emission originates from radiative recombination of delocalized charge carriers after detrapping. Charge carrier separation and release are important processes in colloidal NPLs that strongly affect the excited state dynamics from the subnanosecond to the microsecond time scales.

Methods. *Experimental Details.* Core-only CdSe NPLs were grown following the procedure of Ithurria et al.[2] These were used as seeds to grow CdS crowns and CdS shells following Tessier et al.[5] and Mahler et al.,[3] respectively. Transmission electron microscopy was done on a FEI Tecnai-10 microscope operating at 100 kV. Room-temperature optical measurements were done on NPLs dispersed in anhydrous toluene under nitrogen in an airtight quartz cuvette. Absorption spectra were measured on a double-beam PerkinElmer Lambda 16 UV/vis spectrometer. Emission spectra and PL decay curves were recorded on an Edinburgh Instruments FLS920 spectrofluorimeter. For emission spectra, the NPLs were excited at 400 nm with a 450 W xenon lamp equipped with a double grating monochromator, and recorded on a Hamamatsu R928 photomultiplier tube. PL decay curves and time-resolved emission spectra were obtained by time-correlated single-photon counting on a Hamamatsu H7422-02 photomultiplier tube with low dark count rate (<10 cts/s) and excited with a pulsed laser diode emitting at 441 nm by default (375 nm in Figure 3d) at variable repetition rate. We have not observed an effect of NPL concentration in dispersion on the delayed emission kinetics or intensity on the concentration range investigated between OD $\ll$ 0.01 on the first exciton peak up to OD = 0.3. The excitation fluence is approximately 10^{-7} J cm^{-2}, corresponding to an expectation value of $\langle N \rangle < 0.01$ for the exciton population directly after the pulse (based on the NPL absorption cross-section of $\sigma \approx 10^{-13}$ [44]). For the time-resolved emission maps (Figures 1f and 2e,g), we used a monochromator slit width of 1.5 nm to obtain sufficient signal, possibly leading to some broadening of the narrow NPL emission spectra. The NPL dispersions were not stirred but remained colloidally stable over the course of the measurements. Temperature-dependent measurements were performed with the NPLs drop-casted on an Al_2O_3 coverslip in an Oxford Instruments Microstat-HiResII cryostat, loaded on a Picoquant Microtime 200 confocal microscope, excited with a pulsed laser diode emitting at 402 nm at variable repetition rate, and the PL was detected on a SPAD PDM photodiode.

Fitting the PL Decay Dynamics of NPLs. A power-law distribution of charge carrier release rates $\rho(\gamma) = \gamma^{\alpha-2}$ with lower limit γ_{min} and upper limit γ_{max} gives rise to PL decay with power-law statistics on a time range roughly from γ_{max}^{-1} to γ_{min}^{-1}

$$\int_{\gamma_{min}}^{\gamma_{max}} \gamma\rho(\gamma)e^{-\gamma t}\,d\gamma = At^{-\alpha}[\Gamma(\alpha, \gamma_{min}t) - \Gamma(\alpha, \gamma_{max}t)] \quad (1)$$

where t is the delay time after laser excitation, A is a prefactor that depends on α, γ_{max}, and γ_{min}, and $\Gamma(x, y)$ is the incomplete Gamma function. As in ref 24, for spherical quantum dots, we can fit the PL decay dynamics of core–shell NPLs to an exponential contribution (due to prompt exciton decay) with rate γ_0 and a power-law contribution (due to temporary charge carrier trapping) with $\gamma_{max} = \gamma_0/2$ and $\gamma_{min} = 0$:

$$I(t) = A_0e^{-\gamma_0 t} + A_1t^{-\alpha}\left[\Gamma(\alpha) - \Gamma\left(\frac{\alpha, \gamma_0 t}{2}\right)\right] \quad (2)$$

The PL decay of core-only and core–crown shows two power-law components with different slopes α_1 and α_2

$$I(t) = A_0e^{-\gamma_0 t} + A_1t^{-\alpha_1}\left[\Gamma(\alpha_1, \gamma_1 t) - \Gamma\left(\frac{\alpha, \gamma_0 t}{2}\right)\right] + A_2t^{-\alpha_2}[\Gamma(\alpha_2) - \Gamma(\alpha_2, \gamma_1 t)], \quad (3)$$

where the parameter γ_1 is the decay rate at which the rate distribution changes from power-law with slope (α_1-2) to slope (α_2-2).

■ ASSOCIATED CONTENT

Supporting Information

The Supporting Information is available free of charge on the ACS Publications website at DOI: 10.1021/acs.nanolett.6b00053.

S1: Absorption and emission spectra of the three samples. S2: Comparison of Lorentzian and Gaussian fits. S3: Decay curves on semi and double logarithmic scales. S4: Fitted time-dependent line width of the delayed emission spectrum. S5: Multiexponential fits on delayed emission curves. S6: The effect of reversible trapping on the decay curve. S7: The effect of excitation wavelength. S8: Photoluminescence decay dynamics of trap emission. S9: Temperature-dependent measurements on core–crown and core–shell. (PDF)

■ AUTHOR INFORMATION

Corresponding Author

*E-mail: f.t.rabouw@uu.nl.

Present Address

(P.S.) Institut Pasteur, Citech and Unité d'Analyse d'Images Quantitative, 25-28 rue du Dr. Roux, 75015 Paris, France

Notes

The authors declare no competing financial interest.

■ ACKNOWLEDGMENTS

This work is part of the research program of the "Stichting voor Fundamenteel Onderzoek der Materie (FOM)", which is financially supported by the "Nederlandse Organisatie voor Wetenschappelijk Onderzoek (NWO)".

■ REFERENCES

(1) Ithurria, S.; Dubertret, B. *J. Am. Chem. Soc.* **2008**, *130*, 16504–16505.

(2) Ithurria, S.; Bousquet, G.; Dubertret, B. *J. Am. Chem. Soc.* **2011**, *133*, 3070–3077.

(3) Mahler, B.; Nadal, B.; Bouet, C.; Patriarche, G.; Dubertret, B. *J. Am. Chem. Soc.* **2012**, *134*, 18591–18598.

(4) Prudnikau, A.; Chuvilin, A.; Artemyev, M. *J. Am. Chem. Soc.* **2013**, *135*, 14476–14479.

DOI: 10.1021/acs.nanolett.6b00053
Nano Lett. 2016, 16, 2047–2053

(5) Tessier, M. D.; Spinicelli, P.; Dupont, D.; Patriarche, G.; Ithurria, S.; Dubertret, B. *Nano Lett.* **2014**, *14*, 207−213.
(6) Ithurria, S.; Tessier, M. D.; Mahler, B.; Lobo, R. P. S. M.; Dubertret, B.; Efros, Al. L. *Nat. Mater.* **2011**, *10*, 936−941.
(7) Naeem, A.; Masia, F.; Christodoulou, S.; Moreels, I.; Borri, P.; Langbein, W. *Phys. Rev. B: Condens. Matter Mater. Phys.* **2015**, *91*, 121302.
(8) Chen, Z.; Nadal, B.; Mahler, B.; Aubin, H.; Dubertret, B. *Adv. Funct. Mater.* **2014**, *24*, 295−302.
(9) Fan, F.; Kanjanaboos, P.; Saravanapavanantham, M.; Beauregard, E.; Ingram, G.; Yassitepe, E.; Adachi, M. M.; Voznyy, O.; Johnston, A. K.; Walters, G.; Kim, G.-H.; Lu, Z.-H.; Sargent, E. H. *Nano Lett.* **2015**, *15*, 4611−4615.
(10) Grim, J. Q.; Christodoulou, S.; Di Stasio, F.; Krahne, R.; Cingolani, R.; Manna, L.; Moreels, I. *Nat. Nanotechnol.* **2014**, *9*, 891−895.
(11) Lhuillier, E.; Dayen, J.-F.; Thomas, D. O.; Robin, A.; Doudin, B.; Dubertret, B. *Nano Lett.* **2015**, *15*, 1736−1742.
(12) Sigle, D. O.; Zhang, L.; Ithurria, S.; Dubertret, B.; Baumberg, J. J. *J. Phys. Chem. Lett.* **2015**, *6*, 1099−1103.
(13) Achtstein, A.; Schliwa, A.; Prudnikau, A.; Hardzei, M.; Artemyev, M. V.; Thomsen, C.; Woggon, U. *Nano Lett.* **2012**, *12*, 3151−3157.
(14) Kunneman, L. T.; Schins, J. M.; Pedetti, S.; Heuclin, H.; Grozema, F. C.; Houtepen, A. J.; Dubertret, B.; Siebbeles, L. D. A. *Nano Lett.* **2014**, *14*, 7039−7045.
(15) Biadala, L.; Liu, F.; Tessier, M. D.; Yakovlev, D. R.; Dubertret, B.; Bayer, M. *Nano Lett.* **2014**, *14*, 1134−1139.
(16) Kunneman, L. T.; Tessier, M. D.; Heuclin, H.; Dubertret, B.; Aulin, Y. V.; Grozema, F. C.; Schins, J. M.; Siebbeles, L. D. A. *J. Phys. Chem. Lett.* **2013**, *4*, 3574−3578.
(17) Baghani, E.; O'Leary, S. K.; Fedin, I.; Talapin, D. V.; Pelton, M. *J. Phys. Chem. Lett.* **2015**, *6*, 1032−1036.
(18) Guzelturk, B.; Erdem, O.; Olutas, M.; Kelestemur, Y.; Demir, H. V. *ACS Nano* **2014**, *8*, 12524−12533.
(19) Rowland, C. E.; Fedin, I.; Zhang, H.; Gray, S. K.; Govorov, A. O.; Talapin, D. V.; Schaller, R. D. *Nat. Mater.* **2015**, *14*, 484−489.
(20) Federspiel, F.; Froehlicher, G.; Nasilowski, M.; Pedetti, S.; Mahmood, A.; Doudin, B.; Park, S.; Lee, J.; Halley, D.; Dubertret, B.; Gilliot, P.; Berciaud, S. *Nano Lett.* **2015**, *15*, 1252−1258.
(21) Tessier, M. D.; Javaux, C.; Maksimovic, I.; Loriette, V.; Dubertret, B. *ACS Nano* **2012**, *6*, 6751−6758.
(22) Tessier, M. D.; Mahler, B.; Nadal, B.; Heuclin, H.; Pedetti, S.; Dubertret, B. *Nano Lett.* **2013**, *13*, 3321−3328.
(23) Olutas, M.; Guzelturk, B.; Kelestemur, Y.; Yeltik, A.; Delikanli, S.; Demir, H. V. *ACS Nano* **2015**, *9*, 5041−5050.
(24) Rabouw, F. T.; Kamp, M.; Van Dijk-Moes, R. J. A.; Gamelin, D. R.; Koenderink, A. F.; Meijerink, A.; Vanmaekelbergh, D. *Nano Lett.* **2015**, *15*, 7718−7725.
(25) Sher, P. H.; Smith, J. M.; Dalgarno, P. A.; Warburton, R. J.; Chen, X.; Dobson, P. J.; Daniels, S. M.; Pickett, N. L.; O'Brien, P. *Appl. Phys. Lett.* **2008**, *92*, 101111.
(26) Jones, M.; Lo, S. S.; Scholes, G. D. *Proc. Natl. Acad. Sci. U. S. A.* **2009**, *106*, 3011−3016.
(27) Sippel, P.; Albrecht, W.; Van der Bok, J. C.; Van Dijk-Moes, R. J. A.; Hannappel, T.; Eichberger, R.; Vanmaekelbergh, D. *Nano Lett.* **2015**, *15*, 2409−2416.
(28) Whitham, P. J.; Knowles, K. E.; Reid, P. J.; Gamelin, D. R. *Nano Lett.* **2015**, *15*, 4045−4051.
(29) Katsaba, A. V.; Fedyanin, V. V.; Ambrozevich, S. A.; Vitukhnovsky, A. G.; Sokolikova, M. S.; Vasiliev, R. B. *Semiconductors* **2015**, *49*, 1323−1326.
(30) Kraus, R. M.; Lagoudakis, P. G.; Rogach, A. L.; Talapin, D. V.; Weller, H.; Lupton, J. M.; Feldmann, J. *Phys. Rev. Lett.* **2007**, *98*, 017401.
(31) Liu, S.; Borys, N. J.; Huang, J.; Talapin, D. V.; Lupton, J. M. *Phys. Rev. B: Condens. Matter Mater. Phys.* **2012**, *86*, 045303.
(32) Ebenstein, Y.; Mokari, T.; Banin, U. *Appl. Phys. Lett.* **2002**, *80*, 4033−4035.
(33) Brokmann, X.; Coolen, L.; Dahan, M.; Hermier, J. P. *Phys. Rev. Lett.* **2004**, *93*, 107403.
(34) Pons, T.; Medintz, I. L.; Farrell, D.; Wang, X.; Grimes, A. F.; English, D. S.; Berti, L.; Mattoussi, H. *Small* **2011**, *7*, 2101−2108.
(35) De Jong, M.; Seijo, L.; Meijerink, A.; Rabouw, F. T. *Phys. Chem. Chem. Phys.* **2015**, *17*, 16959−16969.
(36) Voznyy, O.; Sargent, E. H. *Phys. Rev. Lett.* **2014**, *112*, 157401.
(37) Rabouw, F. T.; Vaxenburg, R.; Bakulin, A. A.; Van Dijk-Moes, R. J. A.; Bakker, H. J.; Rodina, A.; Lifshitz, E.; Efros, Al. L.; Femius Koenderink, A. F.; Vanmaekelbergh, D. *ACS Nano* **2015**, *9*, 10366−10376.
(38) Diroll, B. T.; Turk, M. E.; Gogotsi, N.; Murray, C. B.; Kikkawa, J. M. *ChemPhysChem* **2015**.
(39) Javaux, C.; Mahler, B.; Dubertret, B.; Shabaev, A.; Rodina, A. V.; Efros, Al. L.; Yakovlev, D. R.; Liu, F.; Bayer, M.; Camps, G.; Biadala, L.; Buil, S.; Quelin, X.; Hermier, J.-P. *Nat. Nanotechnol.* **2013**, *8*, 206−212.
(40) Kuno, M.; Fromm, D. P.; Hamann, H. F.; Gallagher, A.; Nesbitt, D. J. *J. Chem. Phys.* **2001**, *115*, 1028−1040.
(41) Shimizu, K. T.; Neuhauser, R. G.; Leatherdale, C. A.; Empedocles, S. A.; Woo, W. K.; Bawendi, M. G. *Phys. Rev. B: Condens. Matter Mater. Phys.* **2001**, *63*, 205316.
(42) Tang, J.; Marcus, R. A. *Phys. Rev. Lett.* **2005**, *95*, 107401.
(43) Pelton, M.; Smith, G.; Scherer, N. F.; Marcus, R. A. *Proc. Natl. Acad. Sci. U. S. A.* **2007**, *104*, 14249−14254.
(44) Yeltik, A.; Delikanli, S.; Olutas, M.; Kelestemur, Y.; Guzelturk, B.; Demir, H. V. *J. Phys. Chem. C* **2015**, *119*, 26768−26775.

DOI: 10.1021/acs.nanolett.6b00053
Nano Lett. 2016, 16, 2047−2053